Optics and Photonics Journal, 2013, 3, 243-247
doi:10.4236/opj.2013.32B057 Published Online June 2013 (http://www.scirp.org/journal/opj)

A Theoretical Study of Light Absorption in Self Assembled Quantum Dots

Tarek A. Ameen, Yasser M. El-Batawy, A. A. Abouelsaood
Department of Engineering Physics and Mathematics, Faculty of Engineering, Cairo University, Giza 12613, Egypt
Email: tarek.amin@aucegypt.edu

Received 2013

ABSTRACT

Self assembled quantum dots have shown a great promise as a leading candidate for infrared detection at room temperature. In this paper, a theoretical model of the absorption coefficient of quantum dot devices is presented. Both of bound to bound absorption and bound to continuum absorption are taken into consideration in this model. This model is based on the effective mass theory and the Non Equilibrium Greens Function (NEGF) formalism. NEGF formalism is used to calculate the bound to continuum absorption coefficient. The results of the model have been compared with a published experimental work and a good agreement is obtained. Based on the presented model, the bound to bound absorption coefficient component is compared to the bound to continuum absorption coefficient component. In addition, the effects of the dot dimensions and electron filling on the bound to continuum absorption coefficient are also investigated. In general, increasing the dot filling increases the absorption and decreasing the dots dimensions will increase the absorption and move the absorption peak towards longer wavelengths.

Keywords: Absorption Coefficients; Non Equilibrium Greens Function; Self Assembled Quantum Dots

1. Introduction

Self assembled quantum dots have attracted the attention due to the promise to improve the performance of many applications, like quantum dot infrared photodetectors (QDIP) [1], [2], and intermediate band solar cells (IBSC) [3]. For the QDIPs, it is reported that due to 3-dimensional confinement of the electrons in the quantum dots, QDIPs should have lower dark current than the conventional photodetectors at the same operating temperature, thus QDIPs can operate at higher temperature with the same signal to noise ratio [1]. Also QDIPs are very sensitive to the normal incidence unlike the QWIP [1]. While for the IBSC it should have higher efficiency than the conventional solar cell [4]. The proposed model is based on the non equilibrium Green's function formulation (NEGF). NEGF formalism provides an approach to study the transport in quantum systems in the presence of open boundary conditions via the concept of self energy [5]. The NEGF formalism was used before for modeling the quantum dot-in-a-well (DWELL) structure [6-8]. This model calculated the responsivity not the absorption coefficient of DWELL structure and in arbitrary units. For calculating the bound to bound absorption coefficient of a self assembled quantum dot, a model was presented for the InAS/GaAs QDIP [9]. This model has led to an important result: for QDIP the in-plane polarized absorption is dominant as long as the dot height is not very small compared to its base radius. This result was confirmed experimentally [10]. There are many models that calculate the bound to bound absorption [9,11], but very little work has been done for the bound to continuum absorption. The intraband absorption coefficient α is an important parameter for the design of different quantum dot applications.

In our model, the effective mass theory is used to build a hermitian Hamiltonian matrix for an isolated self assembled quantum dot. Diagonalizing this matrix gives the bound states and energies. Then, this Hamiltonian matrix with a nonhermitian self energy matrix are used to get the NEGF. Using the NEGF, the continuum states of the system have been calculated. Then, the bound to bound and bound to continuum absorption coefficients are both calculated. A comparison of our model and experimental data of [12] has been done, showing a good agreement.

2. Theoretical Model

A schematic of self assembled quantum dot islands is shown in **Figure 1**. The following assumptions are made:

- The self assembled quantum dot islands are assumed to have ideal conical shape with uniform size.
- Both the effects of the wetting layer and the coupling between neighboring dots are neglected.

These assumptions are justified from the scanning probe microscopy done to the self assembled dots [13]. Modeling the absorption coefficient α for quantum dots in previous models [9,11] considered only the bound to bound absorption, where the ground state is the one filled with electrons and the excited states are weakly bound and unoccupied by electrons. These models do not include the bound to continuum absorption. For an efficient and accurate model for α, both the bound to bound and the bound to continuum absorption must be considered. The absorption coefficient α can be expressed as

$$\alpha(\omega) = \frac{2\pi\omega n_{dots}}{n'\epsilon_0 C}\sum_{i,f} N_i N_f \left|\underline{d_{fi}}\cdot\hat{\underline{e}}\right|^2 \delta(E_f - E_i - \hbar\omega) \times (F_i - F_f), \quad (1)$$

where ω is the photon angular frequency, n_{dots} is the number of dots per unit volume, the refractive index of the material is n', the speed of light in free space is C, the free space permittivity is ϵ_0, where i and f stand for initial and final states of possible transitions. For the degeneracy of the initial states we multiply by N_i, and for the degeneracy of the final states we multiply by N_f.

F is the probability of having an electron in an energy state, $\hat{\underline{e}}$ is the polarization of the incident light, and $\underline{d_{fi}}$ is the first order dipole moment and is given by

$$\underline{d_{fi}} = q\iiint_V \underline{r}\,\psi_f^*\,\psi_i\, r\,dr\,d\phi\,dz. \quad (2)$$

For the bound to continuum absorption, the initial states ψ_i are the bound states of the dots, and the final states ψ_f are the continuum states in the conduction band.

For the bound to bound absorption, the initial states are the filled bound states of the dot, and the final states are the empty bound states in the dot. The density of states at E_f is taken to be Gaussian function to add the effect of inhomogeneous broadening resulting from the variation in the dot dimensions, and the bound to bound α can be expressed as

$$\alpha(\omega) = \frac{2\pi\omega n_{dots}}{n'\epsilon_0 C}\sum_{i,f} N_i N_f \left|\underline{d_{fi}}\cdot\hat{\underline{e}}\right|^2 \times \frac{1}{\sqrt{2*\pi\sigma}} e^{\frac{-(E-E_f)^2}{2\sigma^2}} \times (F_i - F_f), \quad (3)$$

this is equivalent to the expressions in [9], [11].

As shown in **Figure 1**, the potential U of the dot in the sample has cylindrical symmetry $U(r,z) = 0$ inside the dot and $U(r,z) = V_b$ outside the dot in the barrier region. The effective mass Hamiltonian H takes the following form in the cylindrical coordinates $\underline{r}\,(r,\phi,z)$ [7]:

$$\hat{H} = \frac{-\hbar^2}{2}\left(\frac{1}{r}\frac{\partial}{\partial r}\left(\frac{r}{m_r}\frac{\partial}{\partial r}\right) + \frac{-n^2}{r^2 m_r} + \frac{\partial}{\partial z}\left(\frac{1}{m_z}\frac{\partial}{\partial z}\right)\right) + U(r,z) \quad (4)$$

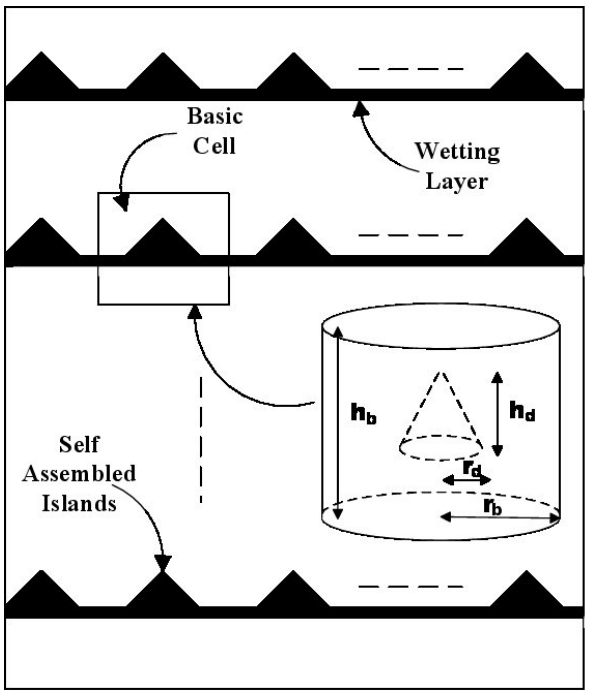

Figure 1. A schematic of the self assembled quantum dot structure.

where m_r is the effective mass in the lateral direction, and m_z is the effective mass in the growth direction, and n is the ϕ quantum number. The discretization of Equation (4) gives the hermitian Hamiltonian matrix H. Diagonalizing this matrix gives the bound state wave functions and energies. For the Continuum states, NEGF is used to include the effects of open boundary conditions. The retarded Green's function G_R of the Hamiltonian operator $\hat{H}$ is given by [5]

$$G^R = \left[(E + i\eta)I - H - \Sigma^R\right]^{-1}\delta, \quad (5)$$

η adds a positive infinitesimal imaginary part to the energy [14]. The self energy matrix Σ^R is given by [5]

$$\Sigma^R = t^2\left[g_l^R(p_i, p_j)\right](r_b\Delta^2),\ t = \frac{-\hbar^2}{2m_{avg}\Delta^2} \quad (6)$$

where t is the coupling coefficient between an element in the basic cell on the boundary and the adjacent element in the lead as shown in **Figure 2**. m_{avg} is the average of the lateral effective mass of electrons between the two materials. $g_l^R(p_i, p_j)$ is a matrix that contains zeros except at the matrix elements between the points p_i, p_j at boundary $r = r_b$ where it equals the retarded Green's function G_{lead}^R just inside the lead. G_{lead}^R is calculated for an isolated lead. A closed form solution for the retarded Green's function in the semi-infinite lead is obtained by solving Equation (5) assuming zero boundary conditions. The result is a series of harmonics and Bessel functions,

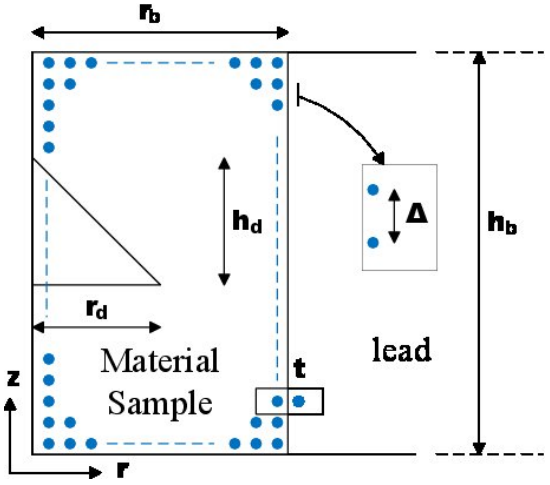

Figure 2. Discretization of the basic cell in the cylindrical coordinates.

$$G^R_{lead} = \sum_l \frac{m_e \pi}{h_b \hbar^2} \sin(k_{zl} z) \sin(k_{zl} z') \frac{H_n^{(1)}(k_{rl}(r_b+\Delta))}{H_n^{(1)}(k_{rl} r_b)} \left(J_n\left(k_{rl}(r_b+\Delta)\right) Y_n(k_{rl} r_b) - J_n(k_{rl} r_b) Y_n\left(k_{rl}(r_b+\Delta)\right)\right) \quad \text{if } E \geq E_l,$$

$$G^R_{lead} = \sum_l \frac{2m_e}{h_b \hbar^2} \sin(k_{zl} z) \sin(k_{zl} z') \frac{K_n(k_{rl}(r_b+\Delta))}{K_n(k_{rl} r_b)} \left(K_n\left(k_{rl}(r_b+\Delta)\right) I_n(k_{rl} r_b) - K_n(k_{rl} r_b) I_n\left(k_{rl}(r_b+\Delta)\right)\right) \quad \text{if } E < E_l, \tag{7}$$

where l is an integer,

$$k_{zl} = \frac{l\pi}{h_b}, E_l = \frac{\hbar^2 k_l^2}{2m_e} + V_b, k_{rl} = \sqrt{\frac{2m_e(E-E_l)}{\hbar^2}}.$$

The continuum wave function of the device is,

$$\psi = -\left[G^R \delta^{-1}\right][S],\ [S] = t[\phi_L(p_i)]. \tag{8}$$

$[S]$ is the source vector which is zeros except at discretization points p_i that are adjacent to the interface with the lead. At these points, $[S]$ is the existing wave function ϕ_L in the lead close to the interface points p_i [5]. The wave function ϕ_L is obtained analytically in the isolated lead with zero boundary conditions. For the infinite end of the lead at ($r \to \infty$), another boundary point $r_L \to \infty$ is added and $\phi_l(r = r_L) = 0$. ϕ_L is obtained by solving Equation (4) using the eigenfunction expansion technique and applying these boundary conditions.

$$\phi_L = \sqrt{\frac{k_r}{h_b r_L (1+C^2)}} \sin(k_{zl} z)\left(J_n(k_r r) - C Y_n(k_r r)\right),$$

$$C = \frac{J_n(k_r r_b)}{Y_n(k_r r_b)},\ k_{zl} = \frac{l\pi}{h_b},\ k_r = \sqrt{\frac{2m_e(E-V_b)}{\hbar^2} - k_{zl}^2} \tag{9}$$

For each mode, the number of continuum states in the mode is determined from the density of states (DOS). The DOS in the continuum spectrum have negligible dependence on the quantum dot. Thus, the number of states N_f with energy E_f in the mode l is calculated in the absence of the dot potential. The device shape becomes a solid disk made from the barrier material with radius r_L and height h_b. N_f is obtained using ordinary DOS calculations,

$$N_f = \frac{m_e r_L}{\pi \hbar^2} \frac{dE_f}{\sqrt{\frac{2m_e}{\hbar^2}(E_f - V_b) - \left(\frac{l\pi}{h_b}\right)^2}} \tag{10}$$

Substituting Equation (10) into Equation (1), the integration

$$\sum_f \delta(E_f - E_i - \hbar\omega) dE_f = 1, \text{ as } E_f = E_i + \hbar\omega.$$

3. Results and Conclusions

The model can be used to calculate α for any self assembled quantum dot structure given its band parameters, doping, dot dimensions r_d, h_d, and the polarization of the incident light $\hat{e}$. The ability to absorb normally incident radiation is an important property to the quantum dot structure, unlike the quantum well structure that is insensitive to the in-plane polarized light. Experimental results have indicated that the normal incidence absorption is more dominant in the quantum dot, unless its height is very small compared to the lateral dimension [10]. So, we will make the calculations for the normally incidence case in this paper.

Calculations have been done for InAs/GaAs quantum dot with dimensions of $r_d = 9.8$ nm and $h_d = 6.3$ nm, where the conduction band offset (CBO) $V_b = 0.321$ eV [15]. **Figure 3** shows the calculated α for the system of InAs/GaAs material with the number of dots per unit volume $n_{dots} = 1.25*10^{21}\,\mathrm{m}^{-3}$ at different values of filling. As shown in this figure, the bound to continuum absorption increases when the excited states are not empty, as the dipole moment from excited states is much greater than the dipole moment from the ground state. Also the bound to bound absorption has greater peak and smaller band width than the bound to continuum absorption. The greater the variations in the dot dimensions, the greater the broadening in the bound to bound absorption. For the bound to bound absorption to occur the dot dimensions must be large enough to have at least one excited state. To see the effect of changing the dot dimensions, calculations are made for different dot dimensions with 2 electrons per dot. **Figure 4** shows the effect of changing the dot radius r_d on the bound to continuum absorption coefficient at $h_d = 6.3$ nm. As shown in this figure,

decreasing the dot radius increases the absorption peak and moves it towards less photon energy. This happens because decreasing the dot radius increases the bound state energies getting them closer to the conduction band which increases the dipole moment. **Figure 5** shows the effect of changing the dot height h_d on the bound to continuum absorption coefficient at $r_d = 9.8$ nm. Also, decreasing the dot height increases the absorption peak and moves it towards less photon energy for the same reason.

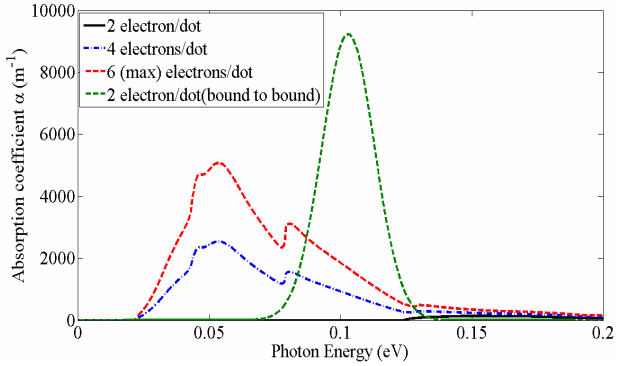

Figure 3. Absorption coefficient α for different cases of electron filling calculated for dot with h_d = 6.3 nm, r_d = 9.8 nm calculated for normal incidence.

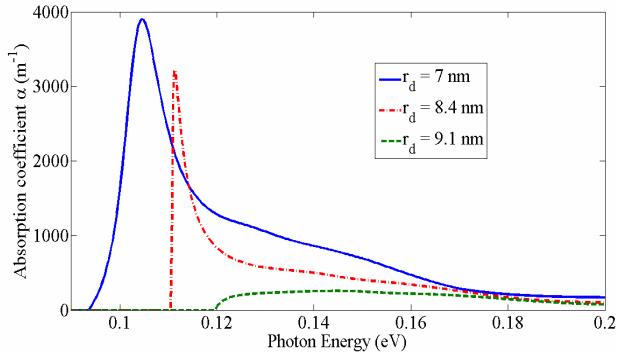

Figure 4. Absorption coefficient α for different values of r_d at h_d = 6.3 nm and 2 electrons per dot.

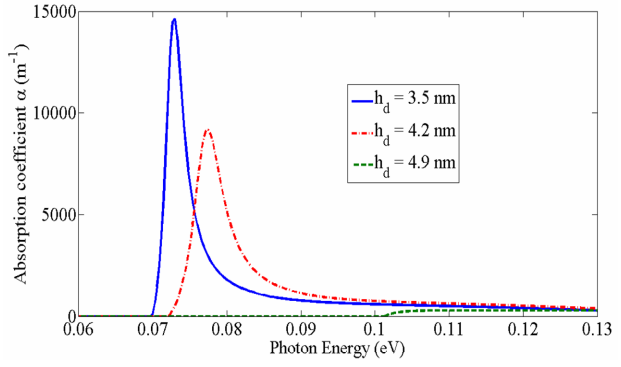

Figure 5. Absorption coefficient α for different values of h_d at r_d = 9.8 nm and 2 electrons per dot.

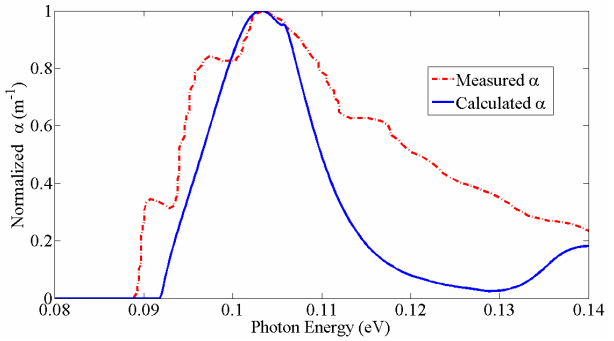

Figure 6. Measured and calculated α for InGaAs/GaAs uncoupled system measured in [10].

To check the validity of our model, we have calculated the bound to continuum absorption coefficient α for an InGaAs/GaAs uncoupled self assembled quantum dots that is measured experimentally in [10]. The calculated results show a very good agreement with the experimental measurements. However the measurements are normalized and the paper doesn't state the number of dots in the studied sample, we made the calculations assuming number of dots $n_{dots} = 1.25*10^{21}\,\mathrm{m}^{-3}$. **Figure 6** shows the measured and calculated α together. In the final analysis, the bound to continuum absorption coefficient becomes much greater as the electron filling in the dot increases. Also decreasing the dot dimensions will increase the absorption and move the absorption peak towards greater wavelengths with higher peaks. On the other hand, the bound to bound absorption occurs at the energy difference between the bound states and it is inhomogeneously broadened by variations in the dot dimensions. The bound to bound is more peaky and larger in value than the bound to continuum absorption coefficient. But if there are no excited states or the excited states are filled with electrons, there will be no bound to bound absorption.

REFERENCES

[1] M. Razeghi, "Technology of Quantum Devices," Springer, 2010. doi:10.1007/978-1-4419-1056-1

[2] P. Martyniuk and A. Rogalski, "Quantum-Dot Infrared Photodetectors: Status and Outlook," *Progress in Quantum Electronics*, Vol. 32, No. 34, 2008, pp. 89–120. doi:10.1142/S0217984908016893

[3] A. L. L. Ana Beln Cristbal Lpez and A. Mart Vega, "Next Generation of Photovoltaics," Springer, 2012. doi:10.1007/978-3-642-23369-2

[4] A. Mart, N. Lpez, E. Antoln, E. Cnovas, C. Stanley, C. Farmer,L. Cuadra, and A. Luque, "Novel Semiconductor Solar Cell Structures: The Quantum Dot Intermediate Band Solar Cell," *Thin Solid Films*, Vol. 511512, pp. 638-644, 2006. doi:10.1016/j.tsf.2005.12.122

[5] S. Datta, "Quantum Transport: Atom to Transistor,"

Cambridge University Press, 2005. doi:10.1017/CBO9781139164313

[6] M. A. Naser, M. J. Deen and D. A. Thompson, "Spectral Function of InAs/InGaAs Quantum Dots in A Well Detector Using Green's Function," *Journal of Applied Physics*, Vol. 100, No. 9, 2006, p. 093102. doi:10.1063/1.2372572

[7] M. A. Naser, M. J. Deen and D. A. Thompson, "Spectral Function and Responsivity of Resonant Tunneling and Superlattice Quantum Dot Infrared Photodetectors Using Green's Function," *Journal of Applied Physics*, Vol. 102, No. 8, 2007, p. 083108. doi:10.1063/1.2799075

[8] M. A. Naser, M. J. Deen and D. A. Thompson, "Theoretical Modeling of Dark Current in Quantum Dot Infrared Photodetectors Using Nonequilibrium Green's Functions," *Journal of Applied Physics*, Vol. 104, No. 1, 2008, p. 014511. doi:10.1063/1.2952014

[9] B. Kochman, A. Stiff-Roberts, S. Chakrabarti, J. Phillips, S. Krishna, J. Singh and P. Bhattacharya, "Absorption, Carrier Lifetime, and Gain in InAs-GaAs Quantum-Dot Infrared Photodetectors," *IEEE Journal of Quantum Electronics*, Vol. 39, 2003, pp. 459-467. doi:10.1109/JQE.2002.808169

[10] A. M. Adawi, E. A. Zibik, L. R. Wilson, A. Lemaˆıtre, J. W. Cockburn, M. S. Skolnick, M. Hopkinson, G. Hill, S. L. Liew and A. G. Cullis, "Strong In-Plane Polarized Intraband Absorption in Vertically Aligned Ingaas/gaas Quantum Dots," *Applied Physics Letters*, Vol. 82, No. 20, 2003, pp. 3415–3417. doi:10.1063/1.1575931

[11] K. Lantz and A. Stiff-Roberts, "Calculation of Intraband Absorption Coefficients in Organic/Inorganic Nanocomposites: Effects of Colloidal Quantum Dot Surface Ligand and Dot Size," *IEEE Journal of Quantum Electronics*, Vol. 47, 2011, pp. 1420-1427. doi:10.1109/JQE.2011.2169235

[12] B. Aslan, H. C. Liu, M. Korkusinski, S.-J. Cheng and P. Hawrylak, "Response Spectra from Mid- to Far-Infrared, Polarization Behaviors, and Effects of Electron Numbers in Quantum-Dot Photodetectors," *Applied Physics Letters*, Vol. 82, No. 4, 2003, pp. 630-632. doi:10.1063/1.1540728

[13] H. Lee, H. Park and T. Kim, "Formation Mode of Self-Assembled CdTe Quantum Dots Directly Grown on Gaas Substrates," *Journal of Crystal Growth*, Vol. 291, No. 2, 2006, pp. 442–447. doi:10.1016/j.jcrysgro.2006.03.018

[14] S. Datta, "Electronic Transport in Mesoscopic Systems," Cambridge University Press, 1996. doi:10.1063/1.2807624

[15] I. Vurgaftman, J. R. Meyer and L. R. Ram-Mohan, "Band Parameters for iii–v Compound Semiconductors and Their Alloys," *Journal of Applied Physics*, Vol. 89, No. 11, 2001, pp. 5815–5875. doi:10.1063/1.1368156

